Acta Astronautica 68 (2011) 160–171

Contents lists available at ScienceDirect

Acta Astronautica

journal homepage: www.elsevier.com/locate/actaastro

A fault-tolerant magnetic spin stabilizing controller for the JC2Sat-FF mission

Anton de Ruiter*

Department of Mechanical and Aerospace Engineering, Carleton University, 1125 Colonel By Drive, Ottawa, ON, Canada K1S 5B6

ARTICLE INFO

Article history:
Received 13 October 2009
Received in revised form
6 May 2010
Accepted 21 July 2010
Available online 17 August 2010

Keywords:
Spin stabilization
Magnetic attitude control
Fault tolerant control

ABSTRACT

This paper presents a spin-stabilization algorithm for the Japan Canada Joint Collaboration Satellite-Formation Flying (JC2Sat-FF) mission using magnetic actuation only. It is shown that under a reasonable assumption on the Earth's magnetic field, the resulting control law is asymptotically stabilizing for an axisymmetric spacecraft, even under the failure of up to two magnetic torque rods and magnetic torque rod saturation. It is also stabilizing under quantization. The satellite motion remains stable under control outages, meaning that the error can be reduced by implementing the control intermittently. The effectiveness of the control law is demonstrated using a high fidelity attitude control system simulator for the JC2Sat-FF satellite.

1. Introduction

The Japan Canada Joint Collaboration Satellite-Formation Flying experiment (JC2Sat-FF) is a joint Canadian Space Agency/Japan Aerospace Exploration Agency (CSA/JAXA) technology demonstration mission, consisting of two nano-satellites, weighing not more than 15 kg each [1]. One of the objectives of this mission is to demonstrate the feasibility of maintaining a spacecraft formation using only differential drag as a means of control. The uniqueness of this project is that differential drag will not only be used for formation keeping but also for other mission modes like formation assembly and formation reconfiguration.

For the attitude control system, the satellites are equipped with two sun-sensors, one three-axis magnetometer, three magnetic torque rods and one pitch momentum wheel (aligned with the *Y*-axis in Fig. 1).

As is described in detail in [2], the two satellites will be launched together in a joint stack configuration. Fig. 1 shows the stacked configuration of the satellites. After separation from the launcher, the satellite stack pitch axis is required to point roughly in the orbit normal direction, as shown in Fig. 1, which is critical for intersatellite separation leading to success of the formation flying part of the mission [2]. Given the JC2Sat orbit, which is an approximately noon–midnight sun-synchronous orbit, approximately one-third of each orbit is in eclipse.

During the preliminary power budget analysis, it is identified that this attitude configuration could not be maintained for more than five orbits in the satellite stack configuration. The reason for this is that, as seen in Fig. 1, one of the satellites is shadowed by the other, significantly reducing the power generation capability of that satellite. Therefore, an additional attitude mode is needed, where the satellite stack can be left for longer periods of time prior to intersatellite separation (in order to perform system checkout, etc.) without draining the batteries.

In order to achieve this, a spin-stabilized mode was selected. By spinning the stack at a high enough rate (several times higher than the orbital rate), each satellite has approximately the same amount of power generation per orbit. Additionally, a spin-stabilized configuration is naturally stable, provided the spin-axis is either a major axis or minor axis of inertia (neglecting internal energy dissipation, which is not significant in the stacked satellite configuration

* Tel.: +1 613 520 2600; fax: +1 613 520 5715.
E-mail address: aderuite@mae.carleton.ca

0094-5765/$ - see front matter © 2010 Elsevier Ltd. All rights reserved.
doi:10.1016/j.actaastro.2010.07.012

Nomenclature

$\vec{\mathbf{a}}$	coordinate-free desired pitch axis unit vector
$\boldsymbol{a}$	desired pitch axis unit vector expressed in satellite body coordinates
$\boldsymbol{B}$	Earth magnetic field vector expressed in satellite body coordinates
$\boldsymbol{B}_I$	Earth magnetic field vector expressed in inertial coordinates
$\mathbf{C}$	rotation matrix representing the satellite attitude with respect to an inertial frame
e_{hy}	angular momentum error about the satellite pitch axis
$\boldsymbol{h}$	satellite angular momentum vector expressed in satellite body coordinates
h	total satellite angular momentum
$\tilde{\mathbf{h}}$	satellite angular momentum error vector expressed in satellite body coordinates
$\vec{\mathbf{h}}_d$	coordinate-free desired angular momentum vector
$\boldsymbol{h}_d$	desired angular momentum vector expressed in satellite body coordinates
h_{dw}	desired angular momentum about the satellite pitch axis
h_t	transverse component of the satellite angular momentum
$\mathbf{I}$	satellite moment of inertia matrix expressed in satellite body coordinates
I_t	transverse component of the satellite inertia matrix
I_y	satellite moment of inertia about the axis of symmetry (pitch axis)
k,k_1,k_2	control law gains
$\mathbf{m}$	magnetorquer dipole moment vector expressed in the satellite body frame
$\boldsymbol{m}_{max}$	magnetorquer limit vector
$\mathbf{W}$	diagonal torque rod selector matrix
α_x	x component of the vector $\boldsymbol{\alpha}$
α_y	y component of the vector $\boldsymbol{\alpha}$
α_z	z component of the vector $\boldsymbol{\alpha}$
$\boldsymbol{\omega}$	satellite angular velocity vector expressed in satellite body coordinates
ω_t	transverse component of the satellite angular velocity
$\boldsymbol{\tau}$	external torque vector expressed in satellite body coordinates
$\mathbf{1}$	identity matrix

when all flexible appendages are stowed). Therefore, it would require little control effort to maintain.

As described in [3], the control functions for spin stabilized spacecraft can be divided into three groups: spin control, precession control and nutation control. For the purposes of JC2Sat-FF, all three are required. Despite the fact that spin-stabilization of spacecraft in one of the oldest forms of attitude stabilization, to this author's knowledge, very little (if any) rigorous treatment of the nonlinear problem has been given when the actuation method is magnetic. Historically, the analyses of the control laws have relied on linearization theory or heuristic arguments [3]. All three control functions are not always treated simultaneously. For example, [4] treats only the nutation control problem, providing a rigorous foundation for that aspect. References [5,6] address both the spin-axis and the spin rate

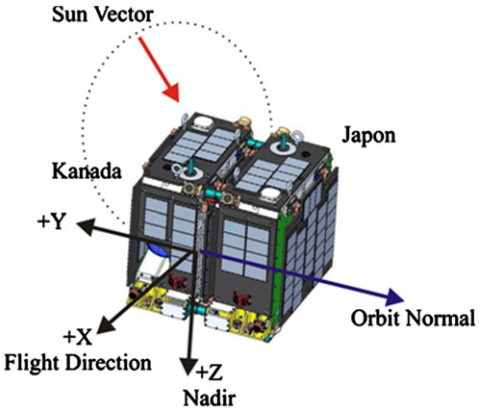

Fig. 1. Satellite joined stack configuration.

control problems but treat them as independent, considering interactions between the two as disturbances.

Reference [3] attempts to address all three control functions simultaneously. It is based upon a Lyapunov approach, where it is shown that $\dot{V}\to 0$ for a Lyapunov function V. However, there are several natural configurations that satisfy $\dot{V}=0$, and the desired configuration is only one of them. Specifically, $\dot{V}=0$ implies that $\boldsymbol{\omega}=\omega_d\boldsymbol{a}$, where ω_d is the desired spin rate about the desired spin axis $\boldsymbol{a}$. This condition can be satisfied by any principal axis spin about the desired spin axis. Assuming that a major axis spin is desired, the condition $\boldsymbol{\omega}=\omega_d\boldsymbol{a}$ is also satisfied by a major axis spin of $-\omega_d$ with the major axis pointing in the direction $-\boldsymbol{a}$. That is, the final configuration is not necessarily the desired one.

In this paper, a magnetic spin-stabilizing control law is presented that simultaneously performs spin-axis, spin rate and nutation control and guarantees that the desired configuration will be obtained. Furthermore, it is shown that under a reasonable assumption on the Earth's magnetic field, the control law is asymptotically stabilizing under the failure of up to two magnetic torque rods, provided the remaining magnetic torque rod is not aligned with the spin axis. It is also stabilizing under quantization. The satellite motion is stable under control outages in the sense that $\dot{V}=0$, that is, the error does not grow. Therefore, the control may be implemented intermittently, reducing the error over time.

Section 2 of this paper details the development of the spin-stabilization control algorithm. The control law is shown to be asymptotically stabilizing under an assumption on the Earth's magnetic field, when attitude and angular velocity measurements are available and ideal. Section 3 examines the assumption made on the Earth's magnetic

field in Section 2. In Section 4, the control algorithm is then implemented in a high fidelity attitude control simulator for the JC2Sat satellite stack and is demonstrated to perform well under realistic conditions (measurement errors, disturbances, non-axisymmetric inertia, etc.), even when two magnetic torque rods are disabled.

The contribution of this paper is then a fault-tolerant magnetic control law for a spin-stabilized spacecraft with provable asymptotic stability, providing simultaneous spin-axis control as well as nutation damping.

2. Mathematical development

This section contains the formulation of the spin-stabilization problem, the mathematical derivation of the control law and the subsequent proof of convergence.

For the purposes of the mathematical development in this section, the spin axis is chosen to be the satellite y-axis. However, it can readily be transformed to any other satellite axis.

2.1. Problem formulation

Let $\vec{\mathbf{a}}$ be a unit vector in the desired body y-axis direction, which is fixed in inertial space. Then, define the desired angular momentum vector to be

$$\vec{\mathbf{h}}_d = h_{dw}\vec{\boldsymbol{a}} \tag{1}$$

where h_{dw} is the desired angular momentum about that axis.[1] Since $\vec{\mathbf{h}}_d$ is fixed in inertial space, in body coordinates, it is governed by

$$\dot{\boldsymbol{h}}_d = -\boldsymbol{\omega}^*\boldsymbol{h}_d \tag{2}$$

where $\boldsymbol{\omega}^* = \begin{bmatrix} 0 & -\omega_z & \omega_y \\ \omega_z & 0 & -\omega_x \\ -\omega_y & \omega_x & 0 \end{bmatrix}$ is the cross product matrix associated with the vector $\boldsymbol{\omega} = \begin{bmatrix} \omega_x & \omega_y & \omega_z \end{bmatrix}^T$ [7, Sect. B.2, p. 526]. The satellite angular momentum in body coordinates is given by $\boldsymbol{h}=\mathbf{I}\boldsymbol{\omega}$ where $\mathbf{I}$ is the satellite moment of inertia matrix. The satellite angular momentum is governed by Euler's equations, which are (see [7, sect. 3.3, p. 59])

$$\dot{\mathbf{h}} = -\boldsymbol{\omega}^*\mathbf{h} + \boldsymbol{\tau} \tag{3}$$

where $\boldsymbol{\tau}$ is the external torque on the satellite. Defining the angular momentum error to be $\tilde{\mathbf{h}} = \mathbf{h} - \mathbf{h}_d$, it also satisfies Euler's equations (from (2) and (3)):

$$\dot{\tilde{\boldsymbol{h}}} = -\boldsymbol{\omega}^*\tilde{\boldsymbol{h}} + \boldsymbol{\tau} \tag{4}$$

The goal is to align the satellite y-axis to coincide with the desired direction $\vec{\mathbf{a}}$. This can be accomplished by first, the angular momentum error $\tilde{\mathbf{h}} = \mathbf{0}$, and second, $h_y = h_{dw}$, where $\mathbf{h} = \begin{bmatrix} h_x & h_y & h_z \end{bmatrix}^T$. For improved control performance, the (seemingly redundant) requirement that $\omega_x = \omega_z = 0$ is added. Since the satellite stack is approximately axisymmetric, the assumption is made that

$$\boldsymbol{I} = \begin{bmatrix} I_x & 0 & 0 \\ 0 & I_y & 0 \\ 0 & 0 & I_z \end{bmatrix} \tag{5}$$

and that $I_x = I_z = I_t$. In this case, Euler's equations become

$$\begin{bmatrix} I_t\dot{\omega}_x \\ I_y\dot{\omega}_y \\ I_t\dot{\omega}_z \end{bmatrix} = \begin{bmatrix} (I_y - I_t)\omega_y\omega_z \\ 0 \\ (I_t - I_y)\omega_x\omega_y \end{bmatrix} + \boldsymbol{\tau} \tag{6}$$

In particular,

$$\dot{h}_y = I_y\dot{\omega}_y = [0 \quad 1 \quad 0]\boldsymbol{\tau} \tag{7}$$

Hence, defining the angular momentum error about the y-axis to be $e_{hy} = h_y - h_{dw}$, this error also satisfies

$$\dot{e}_{hy} = [0 \quad 1 \quad 0]\boldsymbol{\tau} \tag{8}$$

2.2. Derivation of control law

Finally, a suitable control law can be derived. To this end, consider the following Lyapunov-like function:

$$V = \tfrac{1}{2}(\tilde{\mathbf{h}}^T\tilde{\mathbf{h}} + k_1 e_{hy}^2 + k_2\boldsymbol{\omega}^T\boldsymbol{P}\boldsymbol{I}\boldsymbol{\omega}) \tag{9}$$

where $k_1, k_2 > 0$ are gains that can be tuned, and $\mathbf{P} = \mathrm{diag}(1,0,1)$. Since $\mathbf{P}$ and $\mathbf{I}$ are diagonal positive semi-definite, so are their product, $\mathbf{PI}$. The time-derivative of V is readily found to be

$$\dot{V} = (\tilde{\mathbf{h}}^T + k_1 e_{hy}[0 \quad 1 \quad 0] + k_2\boldsymbol{\omega}^T\boldsymbol{P})\boldsymbol{\tau}. \tag{10}$$

With magnetic torque rods, the control torque is given by [7, sect. 8.4, p. 264].

$$\boldsymbol{\tau} = -\mathbf{B}^*\boldsymbol{W}\mathbf{m} \tag{11}$$

where $\mathbf{W}$ selects the available magnetic torque rods. For example, if only x and y axis torque rods are available, then $\mathbf{W} = \mathrm{diag}(1,1,0)$.

The time-derivative of V now becomes

$$\dot{V} = \mathbf{A}^T\mathbf{m} \tag{12}$$

where

$$\mathbf{A} = \boldsymbol{W}\mathbf{B}^*(\tilde{\mathbf{h}} + k_1 e_{hy}[0 \quad 1 \quad 0]^T + k_2\boldsymbol{P}\boldsymbol{\omega}) \tag{13}$$

Based on (12), the control law is chosen to be

$$\mathbf{m} = sat\left[-\frac{k}{\|\mathbf{B}\|^2}\mathbf{A}, \mathbf{m}_{max}\right] \tag{14}$$

where $k > 0$, and the saturation function is defined for the ith component as

$$\{sat[\mathbf{x}, \mathbf{x}_{max}]\}_i = \begin{cases} \{\mathbf{x}\}_i, & |\{\mathbf{x}\}_i| \le \{\mathbf{x}_{max}\}_i \\ \{\mathbf{x}_{max}\}_i \mathrm{sign}(\{\mathbf{x}\}_i), & |\{\mathbf{x}\}_i| > \{\mathbf{x}_{max}\}_i \end{cases} \tag{15}$$

and $\mathbf{m}_{max} = \begin{bmatrix} m_{x\ max} & m_{y\ max} & m_{z\ max} \end{bmatrix}^T$ is the vector of maximum available dipole moment for each magnetic torque rod.

Examining (13) and (14), it can be verified that if all quantities are expressed in terms of SI units, k has unit s^{-1}, k_1 is unitless and k_2 has unit $\mathrm{kg\,m^2}$.

[1] See the nomenclature section.

2.3. Closed-loop stability and convergence

In this section, the closed-loop stability and convergence are examined. First, in Section 2.3.1, it is shown that $\dot{V}\to 0$. Having established this, Section 2.3.2 derives conditions on the control law gains required to establish convergence of the spin-axis and angular velocity errors to zero. In order to do this, two assumptions on the Earth's magnetic field as seen by an orbiting satellite are made. In Section 2.3.3, the second assumption is refined in further detail and its implications for the required active magnetorquers are established.

2.3.1. Convergence of $\dot{V}$

The time derivative of V (in (12)) becomes

$$\dot{V}=-[f(A_x,m_{x\ max})+f(A_y,m_{y\ max})+f(A_z,m_{z\ max})]\le 0 \tag{16}$$

where

$$f(x,x_{max})=\begin{cases}\dfrac{k}{\|\mathbf{B}\|^2}x^2, & \dfrac{k}{\|\mathbf{B}\|^2}|x|<x_{max}\\ |x|x_{max}, & \dfrac{k}{\|\mathbf{B}\|^2}|x|\ge x_{max}\end{cases} \tag{17}$$

Note that $f(x,x_{\max})$ is continuous in x. Since the control input in (14) is continuous in $\tilde{\mathbf{h}}$, e_{hy}, $\boldsymbol{\omega}$ and t, this ensures that the solutions to (4), (6) and (8) ($\tilde{\mathbf{h}}$, e_{hy} and $\boldsymbol{\omega}$, respectively) are continuously differentiable [8, sect. 2.2, p. 67]. The condition (16) together with (9) ensures that they are all bounded. Making use of this fact, Eqs. (4), (6) and (8) all guarantee that $\tilde{\mathbf{h}}$, $\dot{e}_{hy}$ and $\dot{\boldsymbol{\omega}}$ are all bounded as well. Hence, $\tilde{\mathbf{h}}$, e_{hy} and $\boldsymbol{\omega}$ are all bounded and uniformly continuous.

The rotation matrix for the satellite attitude satisfies $\dot{\boldsymbol{C}}=-\boldsymbol{\omega}^*\boldsymbol{C}$. Since $\boldsymbol{\omega}$ is bounded, it can be concluded by the same reasoning as above that C is uniformly continuous as well.

A mild technical assumption on the continuity of the Earth's magnetic field as seen by an orbiting satellite is now required in order to proceed with the convergence analysis.

Assumption 1. It is assumed that the Earth's magnetic field vector (as seen by the orbiting satellite) expressed in the inertial frame $\mathbf{B}_I$ is a uniformly continuous function of time and bounded by $b_1\le|\mathbf{B}_I|\le b_2$ for some $b_2>b_1>0$.

Given the complex nature of the Earth's magnetic field (see [10, sect. 5.1]), it is difficult to verify Assumption 1 in practice. However, it is reasonable to expect that this assumption holds for any spacecraft in a bounded earth orbit.

Assumption 1 leads to both the vectors $\boldsymbol{B}=\boldsymbol{C}\boldsymbol{B}_I$ and finally the product $(k/||\mathbf{B}||^2)\mathbf{A}$ being uniformly continuous and bounded also. Now, let D be a compact interval that contains the elements of the vector $\boldsymbol{A}$. The function $f(x,x_{max})$ is uniformly continuous in x on D, and hence $f(A_x,m_{x\ max})$, $f(A_y,m_{y\ max})$ and $f(A_z,m_{z\ max})$ are uniformly continuous in t. Therefore, from (16), it is concluded that $\dot{V}$ is uniformly continuous in t. Hence, Barbalat's lemma [8, sect. 4.3, p. 192] gives $\dot{V}\to 0$ as $t\to\infty$.

2.3.2. Control law gain constraints

Now, some analysis will be performed to determine suitable gain values in order to guarantee convergence of the spin-axis and angular velocity errors to zero.

Consider the full set of equations describing the closed-loop system. These are the dynamic equations for the spacecraft angular velocity and the dynamic equations for the angular momentum error.

$$\begin{aligned}\boldsymbol{I}\dot{\boldsymbol{\omega}}&=-\boldsymbol{\omega}^*\boldsymbol{I}\boldsymbol{\omega}-\mathbf{B}^*\boldsymbol{W}\mathbf{m}\\ \dot{e}_{hy}&=-[0\quad 1\quad 0]\mathbf{B}^*\boldsymbol{W}\mathbf{m}\\ \dot{\tilde{\mathbf{h}}}&=-\boldsymbol{\omega}^*\tilde{\mathbf{h}}-\mathbf{B}^*\boldsymbol{W}\mathbf{m}\end{aligned} \tag{18}$$

Noting from (14) that $\boldsymbol{m}$ is never orthogonal to $\boldsymbol{A}$ due to the way the control law is designed, it must be that $\dot{V}\to 0\Rightarrow\mathbf{m}\to\mathbf{0}$ and $\mathbf{A}\to\mathbf{0}$. Therefore, the time-varying term on the right-hand side of the system (18) vanishes asymptotically, i.e. $\mathbf{B}^*\boldsymbol{W}\mathbf{m}\to\mathbf{0}$ as $t\to\infty$. Therefore, the system (18) is asymptotically autonomous to the unforced system along any trajectory, and the positive limit set of this trajectory is invariant under the unforced dynamics, and any trajectory of the system approaches this set [9] (see the Appendix). Thus, the trajectories of (18) must approach the largest invariant set of the unforced system contained in the set $G:=\{\tilde{\mathbf{h}},\mathbf{e}_{hy},\boldsymbol{\omega}:\mathbf{A}^T\mathbf{m}=0\}$.

As noted above, $\mathbf{A}^T\mathbf{m}=\dot{V}=0\Rightarrow\mathbf{A}=0$. Thus from (13), unforced invariant solutions are sought that satisfy $\boldsymbol{W}\mathbf{B}^*(\tilde{\mathbf{h}}+k_1e_{hy}[0\quad 1\quad 0]^T+k_2\boldsymbol{P}\boldsymbol{\omega})\equiv 0$. There are two ways in which this may be achieved. The first is that $(\tilde{\mathbf{h}}+k_1e_{hy}[0\quad 1\quad 0]^T+k_2\boldsymbol{P}\boldsymbol{\omega})\equiv 0$. The second is that $\boldsymbol{W}\mathbf{B}^*(\tilde{\mathbf{h}}+k_1e_{hy}[0\quad 1\quad 0]^T+k_2\boldsymbol{P}\boldsymbol{\omega})\equiv 0$ with $(\tilde{\mathbf{h}}+k_1e_{hy}[0\quad 1\quad 0]^T+k_2\boldsymbol{P}\boldsymbol{\omega})\neq 0$.

To proceed, a second technical assumption on the Earth's magnetic field as seen by an orbiting satellite is needed.

Assumption 2. The satellite orbit is such that $\boldsymbol{W}\mathbf{B}^*(\tilde{\mathbf{h}}+k_1e_{hy}[0\quad 1\quad 0]^T+k_2\boldsymbol{P}\boldsymbol{\omega})=0$ with $(\tilde{\mathbf{h}}+k_1e_{hy}[0\quad 1\quad 0]^T+k_2\boldsymbol{P}\boldsymbol{\omega})\neq 0$ is not possible for unforced solutions of (18).

What this assumption means is that it is impossible for the satellite's natural motion to match (in a sense to be made more precise in Section 2.3.3) the time history of the Earth's magnetic field throughout the orbit. This is a reasonable assumption in particular for non-equatorial orbits with significant inclination, since the satellite natural motion contains a small finite number of sinusoidal terms, while the Earth's magnetic field has a number of anomalies (see [10, sect. 5.1]) and is not truly periodic. This assumption is made more precise and examined in more detail in Section 2.3.3.

Proceeding under Assumption 2, the unforced solutions of (18) must satisfy $(\tilde{\mathbf{h}}+k_1e_{hy}[0\quad 1\quad 0]^T+k_2\boldsymbol{P}\boldsymbol{\omega})\equiv 0$. Examining this row by row, it is found that

$$\begin{aligned}&\tilde{\boldsymbol{h}}_x+k_2\boldsymbol{\omega}_x\equiv 0\Rightarrow(I_t+k_2)\boldsymbol{\omega}_x-h_{dw}a_x\equiv 0\\ &\tilde{\boldsymbol{h}}_y+k_1e_{hy}\equiv 0\Rightarrow I_y(1+k_1)\boldsymbol{\omega}_y-h_{dw}(a_y+k_1)\equiv 0\\ &\tilde{\boldsymbol{h}}_z+k_2\boldsymbol{\omega}_z=0\Rightarrow(I_t+k_2)\boldsymbol{\omega}_z-h_{dw}a_z=0\end{aligned} \tag{19}$$

The first and third of these imply that

$$a_x \equiv \frac{(I_t+k_2)}{h_{dw}}\omega_x,$$
$$a_z \equiv \frac{(I_t+k_2)}{h_{dw}}\omega_z. \tag{20}$$

The second condition in (19) implies that

$$a_y \equiv \frac{I_y(k_1+1)}{h_{dw}}\omega_y - k_1 \tag{21}$$

From the unforced system dynamics, $I_y\dot{\omega}_y = 0$, which means that ω_y=constant. From the second condition above, this implies that a_y=constant also. Now, dividing (2) by h_d, the dynamical equations for the desired angular momentum direction are given by ($\dot{\mathbf{a}} = -\boldsymbol{\omega}^*\mathbf{a}$)

$$\begin{aligned}\dot{a}_x &= a_y\omega_z - a_z\omega_y\\ \dot{a}_y &= a_z\omega_x - a_x\omega_z\\ \dot{a}_z &= a_x\omega_y - a_y\omega_x\end{aligned} \tag{22}$$

Substituting for a_x and a_z from (20) to (22) gives that $\dot{a}_y = 0$ as required. Now, examine the angular velocity equations. The dynamical equations are given by

$$\begin{aligned}\dot{\omega}_x &= -\frac{(I_t-I_y)}{I_t}\omega_y\omega_z\\ \dot{\omega}_z &= \frac{(I_t-I_y)}{I_t}\omega_y\omega_x\end{aligned} \tag{23}$$

First, consider the case that $\omega_y \neq 0$, and assume that at least one of $a_x \neq 0$ or $a_z \neq 0$. Define $\boldsymbol{\Omega} = ((I_t-I_y)/I_t)\omega_y$. Note that $\Omega \neq 0$ under the assumption that $I_t \neq I_y$. Then, Eq. (23) is readily solved to give

$$\begin{bmatrix}\omega_x\\ \omega_z\end{bmatrix} = \begin{bmatrix}\cos\boldsymbol{\Omega}t & -\sin\boldsymbol{\Omega}t\\ \sin\boldsymbol{\Omega}t & \cos\boldsymbol{\Omega}t\end{bmatrix}\begin{bmatrix}\omega_{x0}\\ \omega_{z0}\end{bmatrix}. \tag{24}$$

With this solution in hand, a_x and a_z can be obtained using (20), (22) and (24). After some work, the solution is obtained:

$$\begin{aligned}a_x &= \left(\frac{a_y}{\boldsymbol{\Omega}-\omega_y}\omega_{x_0} + a_{x_0}\right)\cos\omega_y t\\ &\quad -\left(\frac{a_y}{\boldsymbol{\Omega}-\omega_y}\omega_{z_0} + a_{z_0}\right)\sin\omega_y t - \frac{a_y}{\boldsymbol{\Omega}-\omega_y}\omega_x\\ a_z &= \left(\frac{a_y}{\boldsymbol{\Omega}-\omega_y}\omega_{x_0} + a_{x_0}\right)\sin\omega_y t\\ &\quad +\left(\frac{a_y}{\boldsymbol{\Omega}-\omega_y}\omega_{z_0} + a_{z_0}\right)\cos\omega_y t - \frac{a_y}{\boldsymbol{\Omega}-\omega_y}\omega_z\end{aligned} \tag{25}$$

Note that $\Omega - \omega_y \neq 0$ due to the definition of Ω. From these solutions, it is clear that a constant relationship between $\boldsymbol{\omega}$ and $\boldsymbol{a}$ (as is required by (20)) is only possible if

$$\begin{aligned}a_x &\equiv -\frac{a_y}{\boldsymbol{\Omega}-\omega_y}\omega_x\\ a_z &\equiv -\frac{a_y}{\boldsymbol{\Omega}-\omega_y}\omega_z\end{aligned} \tag{26}$$

Comparing (26) and (20), it is clear that

$$\frac{I_t+k_2}{h_{dw}} = -\frac{a_y}{\boldsymbol{\Omega}-\omega_y} \tag{27}$$

This can be rewritten as

$$h_{dw}I_t a_y - (I_t+k_2)I_y\omega_y = 0 \tag{28}$$

The condition in (21) relating a_y and ω_y can also be rewritten as

$$-h_{dw}a_y + I_y(k_1+1)\omega_y = k_1 h_{dw} \tag{29}$$

These two Eqs. (28) and (29) may be solved to give

$$a_y = \frac{k_1(I_t+k_2)}{I_t k_1 - k_2} \tag{30}$$

By simply choosing k_1 and k_2 such that $a_y > 1$ leads to a contradiction, since $\boldsymbol{a}$ is a unit vector. Thus, this means that by choosing k_1 and k_2 such that

$$\left|\frac{k_1(I_t+k_2)}{I_t k_1 - k_2}\right| > 1 \tag{31}$$

then a_x=a_z=0 and a_y=± 1.

Now consider the case when ω_y=0. This leads to the requirement (from (21)) that

$$a_y = -k_1 \tag{32}$$

By choosing $k_1 > 1$, this is impossible since $\boldsymbol{a}$ is a unit vector. Hence, ω_y=0 is not possible.

Now, examine (31) under the condition $k_1 > 1$ and $k_2 > 0$. First, assume that $I_t k_1 - k_2 > 0$. In this case, $I_t k_1 + k_1 k_2 > I_t k_1 - k_2$. Now, assume that $k_2 - I_t k_1 > 0$. In this case, $2k_1 I_t + k_1 k_2 > k_1 k_2 > k_2$, since $k_1 > 1$, which implies that $I_t k_1 + k_1 k_2 > k_2 - I_t k_1$. Therefore, if $k_1 > 1$ and $k_2 > 0$, then the inequality (31) is automatically satisfied.

Having chosen appropriate gains ($k_1 > 1$ and $k_2 > 0$), there are only two possible configurations the satellite can end up in. These are the y-axis pointing in the correct direction (a_y=1), and the y-axis pointing in the opposite direction (a_y=-1). When a_y=1, (21) gives

$$h_y = h_{dw} \tag{33}$$

as desired, and that the value of the Lyapunov function is a minimum, namely V=0.

When a_y=-1, (21) gives

$$h_y = h_{dw}\frac{(k_1-1)}{(k_1+1)} \tag{34}$$

and the Lyapunov function value is given by

$$V = 2\frac{k_1}{k_1+1}h_{dw}^2 \tag{35}$$

which is not zero. Since $\dot{V} \leq 0$, if the initial value of the Lyapunov function satisfies

$$V(0) < 2\frac{k_1}{k_1+1}h_{dw}^2 \tag{36}$$

the situation a_y=-1 can never be achieved, and the spacecraft will achieve the desired configuration. In general, there is no guarantee that this initial condition (36) will be satisfied. This problem can be circumvented by a maneuver in two stages. If the spacecraft gets stuck in the situation a_y=-1 with h_y=$h_{dw}(k_1-1)/(k_1+1)$, then the control law can be used to drive the y-axis to point at an angle of 90° from the desired direction with the same h_y=$h_{dw}(k_1-1)/(k_1+1)$. It does not matter which direction is chosen, as long as it is at an angle of 90° from the desired direction. This is the first stage of the maneuver. This maneuver can be performed unambiguously by the following reasoning: let the spacecraft initially have a pure angular momentum about the y-axis with value

$h_y = h_{dw}$, and assume that the desired y-axis direction is 90° from the initial direction. Then, the initial value for the Lyapunov function is given by $V = h_{dw}^2 < 2(k_1/(k_1+1))h_{dw}^2$, and the desired pitch axis direction and angular momentum can be achieved unambiguously.

Returning to the original problem, when the first stage is achieved, it is readily calculated that the Lyapunov function value for the original problem is given by $V = h_{dw}^2 < 2(k_1/(k_1+1))h_{dw}^2$, and the y-axis can readily be driven from this point to the desired direction with no possibility of ending up in the wrong configuration. This is the second stage of the maneuver.

From simulations with random starting points, it was found that this intermediate step was not necessary, since the control law almost always drove the y-axis to the desired direction immediately. This intermediate step can be used as a backup if the spacecraft ends up stuck in the wrong configuration.

Remark 1. *First, given that $\dot{V} = \mathbf{A}^T\mathbf{m}$, the only thing that matters for stability is the sign of the dipole moment $\mathbf{m}$. Thus, the closed-loop system is stable in the presence of quantization, linearity errors, etc., as long as the sign of the control is correct. Second, in the absence of control, $\dot{V} = 0$. That is, the satellite motion is stable in the presence of complete control outages such as would occur during eclipse (if a full attitude measurement is not available). This means that even if the control is implemented intermittently, it will result in a net reduction in error.*

Remark 2. *The control gains can be thought of as follows: the gain $k > 0$ is related to overall convergence of the error. It was found that greater k resulted in faster convergence. However, from a practical point of view, it was found that if k was made too large, the control law effectively becomes bang–bang due to the saturation constraints. Surprisingly, this lead to slower convergence in various numerical simulations performed by the author. The gain $k_1 > 1$ is required to ensure that the spin axis converges to the desired axis. It was found that a large value of k_1 was not needed. A value of k_1 between 1 and 2 appeared to work quite well in various numerical simulations performed by the author. The gain $k_2 > 0$ is a nutation damping gain. It was found that while some nutation damping is required for convergence of the angular velocity error to zero, increasing this gain too much resulted in a slower convergence of the spin axis to the desired axis. That is, the controller put too much effort in damping nutation at the expense of spin axis control. As such, it is recommended to keep the gain k_2 small.*

2.3.3. Further refinement of Assumption 2 and its implications for required active magnetorquers

This section provides a more detailed examination of Assumption 2 on the Earth's magnetic field as seen by an orbiting satellite. That is, the case of unforced solutions of (18) satisfying $\boldsymbol{W}\mathbf{B}^*(\tilde{\mathbf{h}} + k_1 e_{hy}[0 \quad 1 \quad 0]^T + k_2\boldsymbol{P}\boldsymbol{\omega}) = 0$ with $(\tilde{\mathbf{h}} + k_1 e_{hy}[0 \quad 1 \quad 0]^T + k_2\boldsymbol{P}\boldsymbol{\omega}) \neq 0$ is examined. Requirements on which magnetorquers must be active for convergence of the errors to zero are also obtained. It is shown that to ensure convergence of the errors to zero, there must be at least one active magnetorquer aligned with an axis that is not the desired spin axis.

Before continuing, note the following:

Given the solution for the angular velocity $\boldsymbol{\omega}(t)$, the satellite attitude is given by $\boldsymbol{C}(t) = \overline{\boldsymbol{C}}(t)\overline{\boldsymbol{C}}_0$, where $\overline{\boldsymbol{C}}(t)$ is some rotation matrix satisfying $\dot{\overline{\boldsymbol{C}}}(t) = -\boldsymbol{\omega}(t)^*\overline{\boldsymbol{C}}(t)$, and the constant part is given by $\overline{\boldsymbol{C}}_0 = \overline{\boldsymbol{C}}^T(0)\boldsymbol{C}(0)$. The solution for the desired axis is given by $\mathbf{a} = \overline{\boldsymbol{C}}(t)\overline{\boldsymbol{C}}^T(0)\mathbf{a}(0)$, since the matrix $\overline{\boldsymbol{C}}(t)\overline{\boldsymbol{C}}^T(0)$ is the state-transition matrix for the system $\dot{\mathbf{a}} = -\boldsymbol{\omega}^*\mathbf{a}$. Denote the matrix $\overline{\boldsymbol{C}}_0 = \begin{bmatrix} c_{11} & c_{12} & c_{13} \\ c_{21} & c_{22} & c_{23} \\ c_{31} & c_{32} & c_{33} \end{bmatrix}$, which is constant.

There are two possible types of unforced natural motion for an axisymmetric rigid satellite (see [7, sect. 4.2]). These are:

1. Inertially fixed ($\boldsymbol{\omega} = \mathbf{0}$).
2. Coning motion ($\omega_x = \omega_t\cos(\boldsymbol{\Omega}t + \varphi), \omega_y = \omega_{y0}$, $\omega_z = \omega_t\sin(\boldsymbol{\Omega}t + \varphi)$).

In actual fact, case 1 is a special case of case 2, but it is worth examining separately.

Define the vector $\mathbf{D} := (\tilde{\mathbf{h}} + k_1 e_{hy}[0 \quad 1 \quad 0]^T + k_2\boldsymbol{P}\boldsymbol{\omega})$. This vector can be written as

$$\mathbf{D} = \begin{bmatrix} d_x \\ d_y \\ d_z \end{bmatrix} = \begin{bmatrix} (I_t + k_2)\omega_x - h_d a_x \\ I_y(1+k_1)\omega_y - h_d(a_y + k_1) \\ (I_t + k_2)\omega_z - h_d a_z \end{bmatrix} \tag{37}$$

To determine requirements on which magnetorquers must be active to ensure convergence of the errors to zero, the cases when only one magnetic torque rod is present are examined. This corresponds to the situations $\mathbf{W}$=diag(1, 0, 0) when only a torque rod on the x-axis is available, $\mathbf{W}$=diag(0, 1, 0) when only a torque rod on the y-axis is available, and $\mathbf{W}$=diag(0, 0, 1) when only a torque rod on the z-axis is available. Hence, the cases of when the individual elements of $\mathbf{B}^*\mathbf{D}$ are zero are examined. The first element of $\mathbf{B}^*\mathbf{D}$ corresponds to a torque rod aligned with the body x-axis, the second element of $\mathbf{B}^*\mathbf{D}$ corresponds to a torque rod aligned with the body y-axis and the third element of $\mathbf{B}^*\mathbf{D}$ corresponds to a torque rod aligned with the body z-axis. For the first element to be zero, it must be that $d_yB_z - d_zB_y = 0$, which means that the projections of $\boldsymbol{B}$ and $\boldsymbol{D}$ onto the y–z plane must either be parallel, or either of the projections zero. For the second element to be zero, it must be that $d_xB_z - d_zB_x = 0$, which means that the projections of $\boldsymbol{B}$ and $\boldsymbol{D}$ onto the x–z plane must either be parallel, or either of the projections zero. For the third element to be zero, it must be that $d_xB_y - d_yB_x = 0$, which means that the projections of $\boldsymbol{B}$ and $\boldsymbol{D}$ onto the x–y plane must either be parallel, or either of the projections zero.

Case 1. Inertially fixed.

This is the simplest case, with $\overline{\boldsymbol{C}}(t) = \boldsymbol{1}$, and the desired pitch axis is constant. Therefore, the vector $\boldsymbol{D}$ becomes

$$\begin{bmatrix} d_x \\ d_y \\ d_z \end{bmatrix} = \begin{bmatrix} -h_d a_{x0} \\ -h_d(a_{y0} + k_1) \\ -h_d a_{z0} \end{bmatrix} \tag{38}$$

and the Earth magnetic field vector in body coordinates becomes

$$\begin{bmatrix} B_x \\ B_y \\ B_z \end{bmatrix} = \begin{bmatrix} c_{11}B_{xi}+c_{12}B_{yi}+c_{13}B_{zi} \\ c_{21}B_{xi}+c_{22}B_{yi}+c_{23}B_{zi} \\ c_{31}B_{xi}+c_{32}B_{yi}+c_{33}B_{zi} \end{bmatrix} \tag{39}$$

where $\mathbf{B} = \begin{bmatrix} B_x & B_y & B_z \end{bmatrix}^T$ and $\mathbf{B}_I = \begin{bmatrix} B_{xi} & B_{yi} & B_{zi} \end{bmatrix}^T$. The projection of the vector $\boldsymbol{D}$ onto any coordinate plane is constant, and therefore if the orbit is such that $\boldsymbol{B}_I$ spans all of R^3 over time (which is the case for orbits of non-zero inclination), then any coordinate plane projection of $\boldsymbol{D}$ cannot be parallel to the same projection of $\boldsymbol{B}$ for all time. To put it more precisely, it is assumed that the spacecraft orbit is such that given a constant vector $\boldsymbol{f}$,

$$\mathbf{B}_I^T\mathbf{f} \equiv 0 \Rightarrow \mathbf{f} = \mathbf{0}. \tag{40}$$

Therefore, the only possibility is for one of the projections of $\boldsymbol{D}$ to be zero. Since $k_1 > 1$, this means that $d_y \neq 0$ (from (38)), and the only possibility for a zero coordinate plane projection is with $a_{x0}=a_{z0}=0$, making the projection of $\boldsymbol{D}$ onto the x–z plane zero. Therefore, if either a torque rod on the x- or z-axes is present, it is impossible for $\boldsymbol{W}\mathbf{B}^*\mathbf{D} = \mathbf{0}$ with some $\mathbf{D} \neq \mathbf{0}$ in the case of an inertially fixed spacecraft; however it is possible if only a torque rod is present on the y-axis.

Since it has been established in this case that having a torque rod on the y-axis only is not sufficient, there is no need to check it any further in any other case. Since the satellite is axi-symmetric about the pitch axis, it is only necessary to check the case of a torque rod aligned with the body x-axis, since the orientation of the x- and z-axes are arbitrary, as long as the body y-axis is aligned with the satellite axis of inertial symmetry. Therefore, the case of a torque rod aligned with the satellite z-axis can be transformed to a torque rod aligned with the satellite x-axis by a transformation of coordinates.

Case 2. General coning motion.

The angular velocity vector is given by

$$\begin{bmatrix} \omega_x \\ \omega_y \\ \omega_z \end{bmatrix} = \begin{bmatrix} \omega_t\cos(\boldsymbol{\Omega}t+\varphi) \\ \omega_{y0} \\ \omega_t\sin(\boldsymbol{\Omega}t+\varphi) \end{bmatrix} \tag{41}$$

where $\boldsymbol{\Omega} = ((I_t - I_y)/I_t)\omega_{y0}$, $\omega_t = (\omega_{x0}^2+\omega_{z0}^2)^{1/2}$ is the satellite transverse angular velocity and ϕ is some phase dependent on ω_{x0} and ω_{z0}.

A matrix satisfying $\dot{\overline{\mathbf{C}}}(t) = -\boldsymbol{\omega}(t)^*\overline{\mathbf{C}}(t)$ can be found after some work to be (see [7, sect. 4.2])

$$\overline{\mathbf{C}}(t) = \begin{bmatrix} \frac{1}{2}\left(\frac{h_y}{h}-1\right)\cos((\boldsymbol{\Omega}-\boldsymbol{\Omega}_p)t+\varphi)+\frac{1}{2}\left(\frac{h_y}{h}+1\right)\cos((\boldsymbol{\Omega}+\boldsymbol{\Omega}_p)t+\varphi) & \frac{h_t}{h}\cos(\boldsymbol{\Omega}t+\varphi) & \dots \\ \frac{-h_t}{h}\cos(\boldsymbol{\Omega}_p t) & \frac{h_y}{h} & \dots \\ \frac{1}{2}\left(\frac{h_y}{h}-1\right)\sin((\boldsymbol{\Omega}-\boldsymbol{\Omega}_p)t+\varphi)+\frac{1}{2}\left(\frac{h_y}{h}+1\right)\sin((\boldsymbol{\Omega}+\boldsymbol{\Omega}_p)t+\varphi) & \frac{h_t}{h}\sin(\boldsymbol{\Omega}t+\varphi) & \dots \\ \dots & \frac{h_t}{h}\sin(\boldsymbol{\Omega}_p t) & \dots \\ \dots & -\frac{1}{2}\left(\frac{h_y}{h}-1\right)\cos((\boldsymbol{\Omega}-\boldsymbol{\Omega}_p)t+\varphi)+\frac{1}{2}\left(\frac{h_y}{h}+1\right)\cos((\boldsymbol{\Omega}+\boldsymbol{\Omega}_p)t+\varphi) & & \end{bmatrix} \tag{42}$$

where $h = (h_x^2+h_y^2+h_z^2)^{1/2}$ is the satellite total angular momentum, $h_t = (h_x^2+h_z^2)^{1/2}$ is the satellite transverse angular momentum, $\boldsymbol{\Omega}_p = (h/I_t)$ is the precession rate [7, sect. 4.2, p. 100] and φ is some phase angle.

It is useful to define the quantity $\overline{\mathbf{a}}_\mathbf{0} = \begin{bmatrix} \overline{a}_{x0} \\ \overline{a}_{y0} \\ \overline{a}_{z0} \end{bmatrix} = \overline{\mathbf{C}}^T(0)\mathbf{a}(\mathbf{0})$. If only a torque rod aligned with the body x-axis is present, for $\boldsymbol{W}\mathbf{B}^*\mathbf{D} = \mathbf{0}$ to be true, the equality $d_yB_z - d_zB_y = 0$ must be satisfied.

After much algebra, it can be obtained that

$$\begin{aligned} d_yB_z - d_zB_y = \mathbf{B}_I^T\Bigg[& w_1\left(\overline{a}_{x0}\begin{bmatrix} c_{31} \\ c_{32} \\ c_{33} \end{bmatrix} - \overline{a}_{z0}\begin{bmatrix} c_{11} \\ c_{12} \\ c_{13} \end{bmatrix}\right)\cos(\boldsymbol{\Omega}t+\varphi) \\ & + w_2\begin{bmatrix} c_{21} \\ c_{22} \\ c_{23} \end{bmatrix}\sin(\boldsymbol{\Omega}t+\varphi) - \left(w_3\overline{a}_{z0}\begin{bmatrix} c_{21} \\ c_{22} \\ c_{23} \end{bmatrix} + w_4\begin{bmatrix} c_{31} \\ c_{32} \\ c_{33} \end{bmatrix}\right) \\ & \times\cos((\boldsymbol{\Omega}-\boldsymbol{\Omega}_p)t+\varphi) + \left(w_3\overline{a}_{x0}\begin{bmatrix} c_{21} \\ c_{22} \\ c_{23} \end{bmatrix} + w_4\begin{bmatrix} c_{11} \\ c_{12} \\ c_{13} \end{bmatrix}\right) \\ & \times\sin((\boldsymbol{\Omega}-\boldsymbol{\Omega}_p)t+\varphi) + \left(w_5\overline{a}_{z0}\begin{bmatrix} c_{21} \\ c_{22} \\ c_{23} \end{bmatrix} + w_6\begin{bmatrix} c_{31} \\ c_{32} \\ c_{33} \end{bmatrix}\right) \\ & \times\cos(\boldsymbol{\Omega}+\boldsymbol{\Omega}_p)t+\varphi) + \left(w_5\overline{a}_{x0}\begin{bmatrix} c_{21} \\ c_{22} \\ c_{23} \end{bmatrix} + w_6\begin{bmatrix} c_{11} \\ c_{12} \\ c_{13} \end{bmatrix}\right) \\ & \times\sin(\boldsymbol{\Omega}+\boldsymbol{\Omega}_p)t+\varphi)\Bigg] = 0 \end{aligned} \tag{43}$$

where

$$w_1 = \frac{h_d h_t}{h}, w_2 = (I_y(1+k_1)\omega_{y0} - h_d k_1)\frac{h_t}{h} - (I_t+k_2)\frac{\omega_t h_y}{h},$$

$$w_3 = \frac{1}{2}\left[\left(\frac{h_y}{h}-1\right)\frac{h_d h_y}{h} + h_d\left(\frac{h_t}{h}\right)^2\right],$$

$$w_4 = \frac{1}{2}\left[\left(\frac{h_y}{h}-1\right)\left(I_y(1+k_1)\omega_{y0} - h_d k_1 - \frac{h_d h_y}{h}\overline{a}_{y0}\right)\right.$$

$$+\frac{h_t}{h}\left((I_t+k_2)\omega_t-\frac{h_d h_t}{h}\bar{a}_{y0}\right)\Big],$$

$$w_5=\frac{1}{2}\left[\left(\frac{h_y}{h}+1\right)\frac{h_d h_y}{h}+h_d\left(\frac{h_t}{h}\right)^2\right],$$

$$w_6=\frac{1}{2}\left[\left(\frac{h_y}{h}+1\right)\left(I_y(1+k_1)\omega_{y0}-h_d k_1-\frac{h_d h_y}{h}\bar{a}_{y0}\right)+\frac{h_t}{h}\left((I_t+k_2)\omega_t-\frac{h_d h_t}{h}\bar{a}_{y0}\right)\right]$$

Equality (43) has the form

$$\mathbf{B}_I^T\left[\mathbf{f}\cos(\boldsymbol{\Omega}t+\varphi)+\mathbf{g}\sin(\boldsymbol{\Omega}t+\varphi)+\mathbf{h}\cos((\boldsymbol{\Omega}-\boldsymbol{\Omega}_p)t+\varphi)+\mathbf{k}\sin((\boldsymbol{\Omega}-\boldsymbol{\Omega}_p)t+\varphi)+\mathbf{l}\cos((\boldsymbol{\Omega}+\boldsymbol{\Omega}_p)t+\varphi)+\mathbf{n}\sin((\boldsymbol{\Omega}+\boldsymbol{\Omega}_p)t+\varphi)\right]\equiv 0 \tag{44}$$

for some vectors **f**, **g**, **h**, **k**, **l** and **n**. Based on (45), it is assumed that the orbit is such that given any Ω, Ω_p and ϕ, the equality (44) is the only possibility provided

$$\left[\mathbf{f}\cos(\boldsymbol{\Omega}t+\varphi)+\mathbf{g}\sin(\boldsymbol{\Omega}t+\varphi)+\mathbf{h}\cos((\boldsymbol{\Omega}-\boldsymbol{\Omega}_p)t+\varphi)+\mathbf{k}\sin((\boldsymbol{\Omega}-\boldsymbol{\Omega}_p)t+\varphi)+\mathbf{l}\cos((\boldsymbol{\Omega}+\boldsymbol{\Omega}_p)t+\varphi)+\mathbf{n}\sin((\boldsymbol{\Omega}+\boldsymbol{\Omega}_p)t+\varphi)\right]\equiv 0 \tag{45}$$

There are now several subcases to be examined. These are:

(a) $\boldsymbol{\Omega}=\boldsymbol{\Omega}_p=0$
(b) $\Omega\neq 0$, $\Omega_p\neq 0$, $\Omega\neq\pm 2\Omega_p$, $h_t\neq 0$
(c) $\boldsymbol{\Omega}>0$, $\boldsymbol{\Omega}_p=2\boldsymbol{\Omega}$, $h_t\neq 0$
(d) $\Omega<0$, $\Omega_p=-2\Omega$, $h_t\neq 0$
(e) $\boldsymbol{\Omega}=0$, $\boldsymbol{\Omega}_p\neq 0$
(f) $h_t=0$, $h_y\neq 0$

Note that due to the definitions of Ω_p and Ω, $|\Omega|<\Omega_p$, so that it is impossible to have $\Omega_p=0$, $\Omega\neq 0$ or $\Omega=\pm\Omega_p$. These are now examined case by case.

Case a.

The condition $\Omega=\Omega_p=0$ implies that $h=0$, which means that the spacecraft is inertially fixed. This case has already been treated separately.

Case b.

Making use of the fact that the columns of $\overline{\mathbf{C}}_o$ are mutually orthogonal unit vectors, with $\Omega\neq 0$, $\Omega_p\neq 0$, $\Omega_p\neq\pm 2\Omega$, Eq. (43) under the assumption in (45) leads to the requirement that $w_2=w_4=w_6=0$ and either $\bar{a}_{x0}=\bar{a}_{z0}=0$ or $w_1=w_3=w_5=0$. The condition $h_t\neq 0$ means that $w_1\neq 0$, which implies that $\bar{a}_{x0}=\bar{a}_{z0}=0$ and consequently $\bar{a}_{y0}=\pm 1$. $w_4=w_6=0$ leads to the equalities:

$$\left(I_y(1+k_1)\omega_{y0}-h_d k_1-\frac{h_d h_y}{h}\bar{a}_{y0}\right)=0 \tag{46}$$

and

$$\left((I_t+k_2)\omega_t-\frac{h_d h_t}{h}\bar{a}_{y0}\right)=0 \tag{47}$$

Since $\omega_t>0$ by definition, from (47), it must be that the product $h_d\bar{a}_{y0}>0$. Therefore, since $\bar{a}_{y0}=\pm 1$, $h_d\bar{a}_{y0}=|h_d|$. Eq. (47) can consequently be solved to give

$$h=\frac{I_t|h_d|}{(I_t+k_2)} \tag{48}$$

Substituting (48) into (46) leads to

$$|h_y|=\left|\frac{k_1(I_t+k_2)}{I_t k_1-k_2}\right|h \tag{49}$$

Now, from (31), this leads to

$$|h_y|>h, \tag{50}$$

which is impossible since $h=(h_y^2+h_t^2)^{1/2}$.

Case c

The situation $\Omega>0$, $\Omega_p=2\Omega$, $h_t\neq 0$, gives $\Omega-\Omega_p=-\Omega$. Substituting this into (44) the following equalities can be obtained:

$$-w_1\bar{a}_{z0}\cos\varphi+w_4\sin\varphi=0 \tag{51}$$

$$w_1\bar{a}_{x0}\cos\varphi-w_4\cos\varphi=0 \tag{52}$$

$$w_1\bar{a}_{z0}\sin\varphi-w_4\cos\varphi=0 \tag{53}$$

$$-w_1\bar{a}_{x0}\sin\varphi-w_4\sin\varphi=0 \tag{54}$$

$$w_6=0 \tag{55}$$

After some work, the equalities (51)–(55) lead to the requirement that $w_4=w_6=0$ and $\bar{a}_{x0}=\bar{a}_{z0}=0$. Consequently $\bar{a}_{y0}=\pm 1$. These are the exact same conditions as for case b, which is impossible.

Case d.

The situation $\Omega<0$, $\Omega_p=-2\Omega$, $h_t\neq 0$, gives $\Omega-\Omega_p=-\Omega$. Substituting this into (43) and making use of the assumption in (45), the following equalities can be obtained:

$$-w_1\bar{a}_{z0}\cos\varphi+w_6\sin\varphi=0 \tag{56}$$

$$w_1\bar{a}_{x0}\cos\varphi+w_6\cos\varphi=0 \tag{57}$$

$$w_1\bar{a}_{z0}\sin\varphi-w_6\cos\varphi=0 \tag{58}$$

$$-w_1\bar{a}_{x0}\sin\varphi+w_6\sin\varphi=0 \tag{59}$$

$$w_4=0 \tag{60}$$

As for case c, the equalities (56)–(60) lead to the requirement that $w_4=w_6=0$ and $\bar{a}_{x0}=\bar{a}_{z0}=0$. Consequently $\bar{a}_{y0}=\pm 1$. These are the exact same conditions as for case b, which is impossible.

Case e.

This is a special case of a pure spin about an axis orthogonal to the body y-axis. From the definition of Ω, it is obtained that $h_y=0$ and therefore $h=h_t$, and from the definition of Ω_p, $h\neq 0$. In this case, the coefficients defined in (43) become

$$\begin{aligned}
w_1&=h_d\\
w_2&=-h_d k_1\\
w_3&=\tfrac{1}{2}h_d\\
w_4&=\tfrac{1}{2}\left[h_d k_1+(I_t+k_2)\omega_t-h_d\bar{a}_{y0}\right]\\
w_5&=\tfrac{1}{2}h_d\\
w_6&=\tfrac{1}{2}\left[-h_d k_1+(I_t+k_2)\omega_t-h_d\bar{a}_{y0}\right]
\end{aligned} \tag{61}$$

With $\Omega=0$, the constant part of (43) leads to the requirement that

$$w_1[\bar{a}_{x0}c_3-\bar{a}_{z0}c_1]\cos\varphi+w_2c_2\sin\varphi=0, \tag{62}$$

Since $w_2\neq 0$, this leads to $\sin\phi=0$, and subsequently since $w_1\neq 0$ and $\cos\phi\neq 0$, this leads to $\bar{a}_{x0}=\bar{a}_{z0}=0$ and

consequently $\bar{a}_{y0} = \pm 1$. With $\sin\phi = 0$, making use of double angle formulae the periodic terms in (43) become

$$\cos((\boldsymbol{\Omega}-\boldsymbol{\Omega}_p)t+\varphi) = \cos\varphi\cos\boldsymbol{\Omega}_p t$$
$$\sin((\boldsymbol{\Omega}-\boldsymbol{\Omega}_p)t+\varphi = -\cos\varphi\sin\boldsymbol{\Omega}_p t$$
$$\cos((\boldsymbol{\Omega}+\boldsymbol{\Omega}_p)t+\varphi = \cos\varphi\cos\boldsymbol{\Omega}_p t$$
$$\sin((\boldsymbol{\Omega}+\boldsymbol{\Omega}_p)t+\varphi = \cos\varphi\sin\boldsymbol{\Omega}_p t \tag{63}$$

Making use of (63) and the fact that $\bar{a}_{x0} = \bar{a}_{z0} = 0$, Eq. (43) under the assumption in (45) leads to the condition

$$c_3[w_4+w_6]\cos\varphi\cos\boldsymbol{\Omega}_p t + c_1[w_6-w_4]\cos\varphi\cos\boldsymbol{\Omega}_p t = 0 \tag{64}$$

which leads to the requirement that

$$w_4 = w_6 = 0. \tag{65}$$

However, from (62), w_4=w_6 implies that h_d=$-h_d$, which is not true, since $h_d \neq 0$ by definition.

Case f.

The condition h_t=0, $h_y \neq 0$ denotes a pure spin about the spacecraft body y-axis. In this case, h=$|h_y| \neq 0$, and the coefficients in (43) become

$$w_1 = 0$$
$$w_2 = 0$$
$$w_3 = \tfrac{1}{2}h_d(1 \mp 1)$$
$$w_4 = \tfrac{1}{2}(\pm 1-1)\left[I_y(1+k_1)\omega_{y0} - h_d k_1 \pm h_d\bar{a}_{y0}\right]$$
$$w_5 = \tfrac{1}{2}h_d(1 \pm 1)$$
$$w_6 = \tfrac{1}{2}(\pm 1+1)\left[I_y(1+k_1)\omega_{y0} - h_d k_1 \pm h_d\bar{a}_{y0}\right] \tag{66}$$

From (66), it must be that either w_3=0 or w_5=0. Now, if w_3=0, then w_4=0 and $w_5 \neq 0$. From (45) this leads to

$$(w_5\bar{a}_{z0}c_2 + w_6c_3)\cos((\boldsymbol{\Omega}+\boldsymbol{\Omega}_p)t+\varphi) + (w_5\bar{a}_{x0}c_2 + w_6c_1)\sin((\boldsymbol{\Omega}+\boldsymbol{\Omega}_p)t+\varphi) = 0 \tag{67}$$

Now, w_3=0 results from $h_y > 0$, in which case it can be shown that Ω+Ω_p=ω_{y0}. Therefore, (67) leads to $\bar{a}_{x0} = \bar{a}_{z0} = w_6 = 0$, which also means that $\bar{a}_{y0} = \pm 1$. The rotation matrix in (42) becomes

$$\overline{\mathbf{C}}(t) = \begin{bmatrix} \cos(\omega_y t+\varphi) & 0 & -\sin(\omega_y t+\varphi) \\ 0 & 1 & 0 \\ \sin(\omega_y t+\varphi) & 0 & \cos(\omega_y t+\varphi) \end{bmatrix} \tag{68}$$

which leads to a_x=0, a_y=± 1, a_z=0. Therefore, the vector $\boldsymbol{D}$ can be assembled (from (38)) as $\mathbf{D} = \begin{bmatrix} 0 \\ w_6 \\ 0 \end{bmatrix}$, and the requirement that w_6=0 leads to $\mathbf{D} = \mathbf{0}$.

Similarly, if w_5=0, then $w_3 \neq 0$ and w_6=0. From (43) under the assumption in (45),

$$-(w_3\bar{a}_{z0}c_2 + w_4c_3)\cos((\boldsymbol{\Omega}-\boldsymbol{\Omega}_p)t+\varphi) + (w_3\bar{a}_{x0}c_2 + w_4c_1)\sin((\boldsymbol{\Omega}-\boldsymbol{\Omega}_p)t+\varphi) = 0 \tag{69}$$

Now, w_5=0 results from $h_y < 0$, and it can be shown that $\Omega - \Omega_p$=ω_{y0}. Therefore, equality (69) leads to $\bar{a}_{x0} = \bar{a}_{z0} = w_4 = 0$, which also means that $\bar{a}_{y0} = \pm 1$. The rotation matrix in (44) becomes

$$\overline{\mathbf{C}}(t) = \begin{bmatrix} -\cos(\omega_y t+\varphi) & 0 & -\sin(\omega_y t+\varphi) \\ 0 & -1 & 0 \\ -\sin(\omega_y t+\varphi) & 0 & \cos(\omega_y t+\varphi) \end{bmatrix} \tag{70}$$

which leads to a_x=0, a_y=± 1 and a_z=0.

Therefore, the vector $\boldsymbol{D}$ can be assembled (from (38)) as $\mathbf{D} = \begin{bmatrix} 0 \\ -w_4 \\ 0 \end{bmatrix}$, and the requirement that w_4=0 leads to $\mathbf{D} = \mathbf{0}$.

In conclusion of the preceding analysis, a non-trivial solution to $\boldsymbol{W}\mathbf{B}^*\mathbf{D} = \mathbf{0}$ with $\mathbf{D} \neq \mathbf{0}$ is not possible if there is at least a magnetic torque rod aligned with the body x-axis (or body z-axis) in the case of spacecraft in coning motion, provided (44) is only possible if (45) is true.

In light of the analysis in this section, Assumption 2 can be replaced by

Assumption 2′. There is at least one magnetic torque rod aligned with either the x- or z-axes, and for any Ω, Ω_p and ϕ, the equality

$$\mathbf{B}_l^T\left[\mathbf{f}\cos(\boldsymbol{\Omega}t+\varphi) + \mathbf{g}\sin(\boldsymbol{\Omega}t+\varphi) + \mathbf{h}\cos((\boldsymbol{\Omega}-\boldsymbol{\Omega}_p)t+\varphi) + \mathbf{k}\sin((\boldsymbol{\Omega}-\boldsymbol{\Omega}_p)t+\varphi) + \mathbf{l}\cos((\boldsymbol{\Omega}+\boldsymbol{\Omega}_p)t+\varphi) + \mathbf{n}\sin((\boldsymbol{\Omega}+\boldsymbol{\Omega}_p)t+\varphi)\right] \equiv 0 \tag{71}$$

holds if and only if

$$\left[\mathbf{f}\cos(\boldsymbol{\Omega}t+\varphi) + \mathbf{g}\sin(\boldsymbol{\Omega}t+\varphi) + \mathbf{h}\cos((\boldsymbol{\Omega}-\boldsymbol{\Omega}_p)t+\varphi) + \mathbf{k}\sin((\boldsymbol{\Omega}-\boldsymbol{\Omega}_p)t+\varphi) + \mathbf{l}\cos((\boldsymbol{\Omega}+\boldsymbol{\Omega}_p)t+\varphi) + \mathbf{n}\sin((\boldsymbol{\Omega}+\boldsymbol{\Omega}_p)t+\varphi)\right] \equiv 0 \tag{72}$$

Remark 3. *Given the various anomalies contained in the Earth's magnetic field (see chapter 5 in [10, sect. 5.1]), Assumption 2′ is very reasonable for satellite orbits with non-zero inclination.*

3. Numerical example

In this section, the spin-stabilization controller that is derived in this paper is tested using a high fidelity attitude simulator for the JC2Sat satellite stack, presented in Fig. 1. Only one of the satellites' ACS systems is used to control the stack. The satellite attitude and angular rate are estimated with an extended Kalman filter using two sun-sensors whose fields of view are 70° and one magnetometer. The sun sensors have an accuracy of 0.2°, which is modeled as a bias. A 0.5° sensor misalignment due to mechanical installation is also included. The magnetometer also has a misalignment of 0.5° due to mechanical installation. Additional to this is a 550 nT bias and a normally distributed environmental noise of magnitude 500 nT (RMS).

The simulations include gravity-gradient and residual magnetic disturbance torques with a residual magnetic dipole moment $\boldsymbol{m}_{res} = \begin{bmatrix} 0.1 & -0.1 & 0.1 \end{bmatrix}^T$ Am^2.

The satellite stack is in a sun-synchronous orbit, with local time of descending node 22:30. The altitude is 650 km, with the orbital period being approximately 5864 s, and the satellite being in eclipse for approximately 2000 s per orbit, during which time the satellite sun

sensors are not available. The satellite has three magnetic torque rods, one aligned with each of the satellite body axes. The magnetic torque rods have saturation constraints of $\times 1.75$ Am^2.

The desired spin axis of the JC2Sat stack is the major or minor principal axis closest to the x-axis (see Fig. 1). In order to fit with the control law derived in this paper, a coordinate transformation from body to principal axes is used such that the principal y-axis is the major axis closest to the body x-axis. The desired spin axis direction is the nadir pointing vector at the point of highest latitude of the orbit. The desired spin rate is 5°/s.

Unlike in the preceding analysis, the satellite stack is triaxial with a moment of inertia matrix in body coordinates is

$$\mathbf{I} = \begin{bmatrix} 1.0669 & -0.0258 & 0.0000 \\ -0.0258 & 1.0322 & 0.0033 \\ 0.0000 & 0.0033 & 1.0475 \end{bmatrix} \text{kgm}^2$$

and the rotation matrix from body to principal coordinates is

$$\boldsymbol{C}_{pb} = \begin{bmatrix} -0.4774 & -0.8734 & 0.0962 \\ 0.8741 & -0.4832 & -0.0499 \\ 0.0900 & 0.0603 & 0.9941 \end{bmatrix}$$

The stack moment of inertia matrix in principal coordinates is then

$$\boldsymbol{I}_p = \begin{bmatrix} 1.0178 & 0.0000 & 0.0000 \\ 0.0000 & 1.0792 & 0.0000 \\ 0.0000 & 0.0000 & 1.0477 \end{bmatrix} \text{kgm}^2$$

The initial satellite angular velocity in stack principal coordinates is $\omega_{x,p}(0)$=1.9795°/s, $\omega_{y,p}(0)$=5.2359°/s, $\omega_{z,p}(0)$=4.1513°/s. The initial pointing error is 75.8493°.

The controller gains are $k = 0.004$, $k_1 = 1.5$ and $k_2 = 0.5$.

In order to demonstrate the effectiveness of the controller, two simulations are performed. The first simulation has all three magnetic torque rods active.

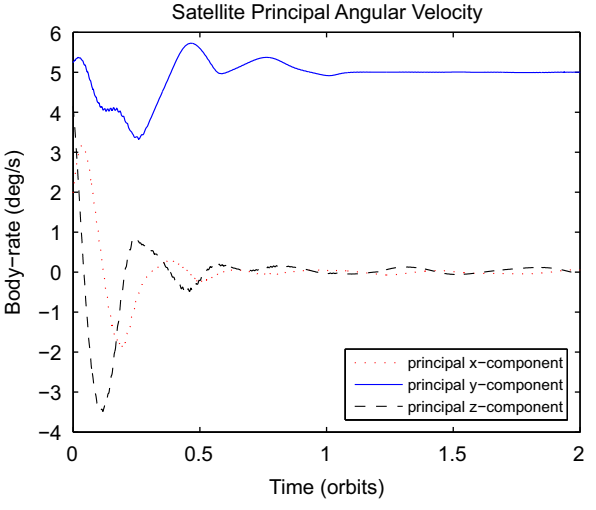

Fig. 2. Stack angular velocity in principal coordinates (three torque rods active).

In the second simulation, the magnetic torque rods aligned with the satellite x- and y- axes are disabled. It will be seen that despite the fact that the satellite stack is triaxial, effective convergence of errors is still obtained in all simulated cases.

The results are presented in Figs. 2–7.

3.1. All magnetic torque rods active

In this section, all three (x- y- and z-axes) magnetic torque rods are active. Fig. 2 shows the satellite stack angular velocity as expressed in principal coordinates. It can be seen that the desired spin rate of 5°/s about the principal y-axis is achieved within a single orbit. Fig. 3 shows the angle between the principal y-axis and its desired direction. It can be seen that the desired spin-axis direction is achieved within a single orbit. Fig. 4 shows the magnetorquer effort.

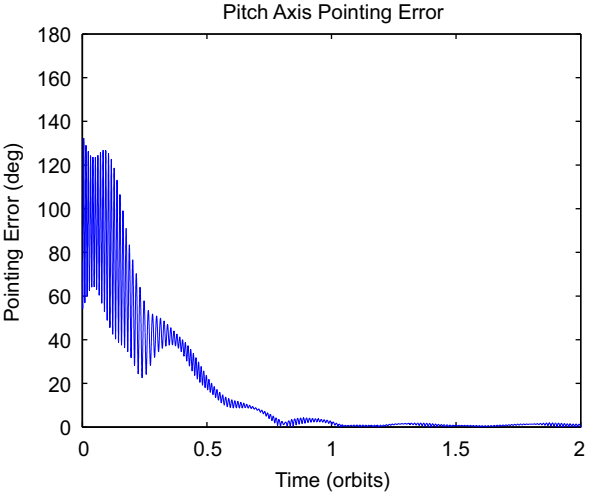

Fig. 3. Pointing error (three torque rods active).

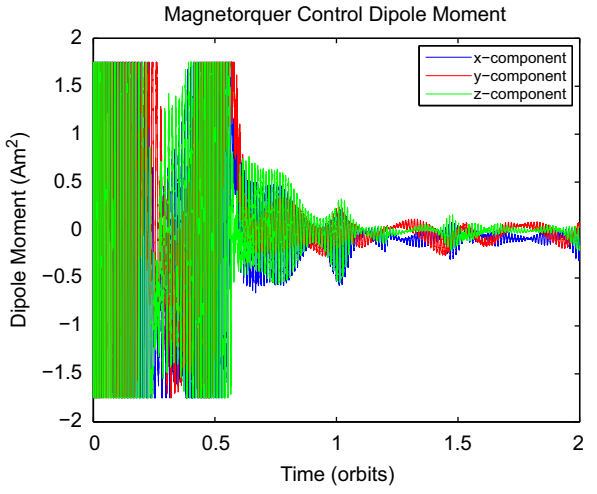

Fig. 4. Magnetictorquer effort.

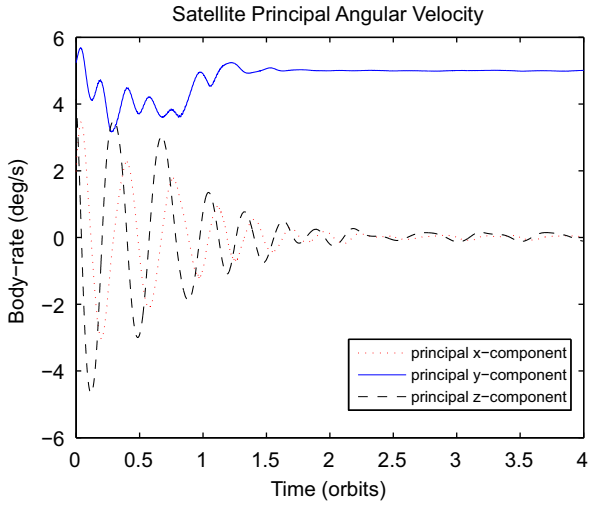

Fig. 5. Stack angular velocity in principal coordinates (x- and y-torque rods disabled).

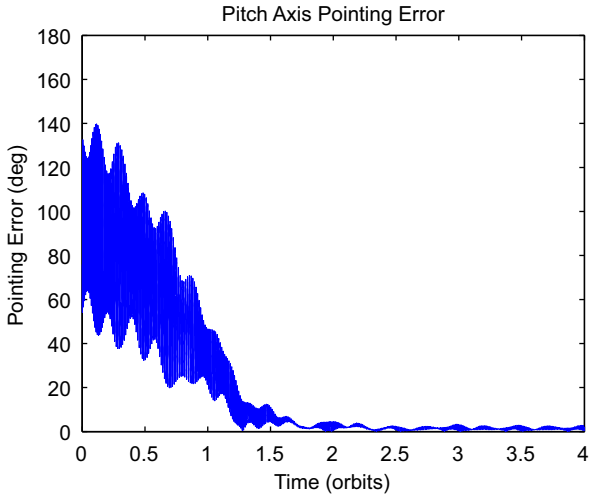

Fig. 6. Pointing error (x- and y-torque rods disabled).

3.2. *x and y torquer disabled*

In this section, the magnetic torque rods aligned with the x- and y-axes are disabled so that the only torque rod available is aligned with the z-axis. It can be seen from Figs. 5 and 6 that the convergence of the attitude is much slower than when all three torquers are enabled (Figs. 2 and 3), but as predicted by the theory, the satellite stack converges to the desired spin rate and direction, which is achieved after approximately two orbits. Fig. 7 shows the magnetorquer effort.

4. Conclusion

This paper has presented a spin-stabilization control law using magnetic actuation. It is shown that under a reasonable assumption on the Earth's magnetic field, the control law is asymptotically stabilizing for an axisymmetric spacecraft under controller saturation and the failure of magnetic torque rods aligned with up to two axes, provided the remaining magnetic torque rod is not aligned with the desired spin axis. It is also stabilizing under quantization effects. During control outages, the errors do not grow. As such, the control law may be implemented intermittently and still achieve a net reduction in error.

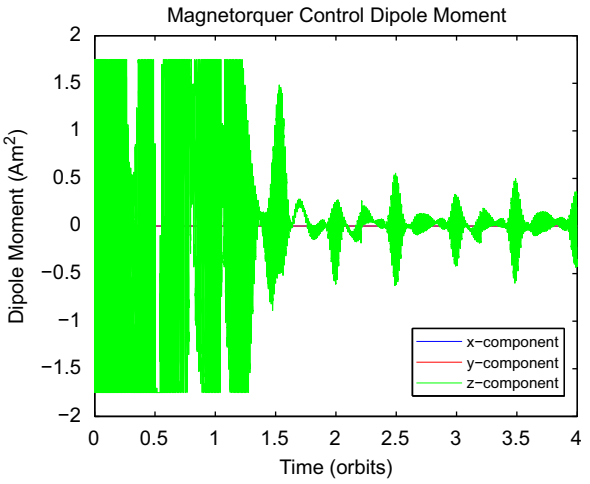

Fig. 7. Magnetictorquer effort.

This control law was developed for the initial phase of the Japan Canada Joint Collaboration Satellite-Formation Flying mission. Its effectiveness is demonstrated on a high fidelity nonlinear attitude simulator for the JC2Sat satellite stack, where it is shown to be asymptotically stable even when a single magnetic torque rod is used. The numerical simulation shows that the control law still performs well when the satellite has triaxial inertia properties.

Acknowledgements

The author gratefully acknowledges the valuable discussions and feedback from James Lee, Yuri Kim and Alfred Ng of the Canadian Space Agency. The author also thanks the reviewers for the many useful comments which helped to greatly improve the paper.

Appendix

This paper makes use of an invariance property for asymptotically autonomous systems. The result used is presented in Lasalle's seminal paper [9] but is not that well known. It is therefore repeated here.

A system of the form

$$\dot{x} = F(x) + g(x,t) \tag{73}$$

is said to be *asymptotically autonomous* if $g(x,t) \to 0$ uniformly in x as $t \to \infty$. As stated in [9], the positive limit sets of solutions of (73) are invariant under $\dot{x} = F(x)$.

As is shown in [9], this property may be applied to systems that are not asymptotically autonomous, but have solutions that are also solutions of asymptotically autonomous systems, as is the case in this paper. The following example is adapted from [9] and demonstrates this principle.

Consider the system

$$\dot{x} = y$$
$$\dot{y} = -x - p(t)y, \quad 0 < p(t) \leq m \tag{74}$$

with $p(t)$ a uniformly continuous function of t. Consider the Lyapunov-like function $V = x^2 + y^2$. Along the trajectories of (74), $\dot{V} = -p(t)y^2 < 0$. Therefore, both x and y are bounded, and from (74), it can be concluded that x and y are uniformly continuous and bounded in t. Therefore, $\dot{V}$ itself is uniformly continuous in t, and it can be concluded from Barbalat's Lemma [8, sect. 4.3, p. 192] that $\dot{V} \to 0$, and hence $y \to 0$ as $t \to \infty$. Now, let $(\bar{x}(t), \bar{y}(t))$ be any solution of (74). This solution also is a solution of the system

$$\dot{x} = y$$
$$\dot{y} = -x - p(t)\bar{y}(t), \quad 0 < p(t) \leq m \tag{75}$$

which is asymptotically autonomous to

$$\dot{x} = y$$
$$\dot{y} = -x \tag{76}$$

Now, positive limit sets of solutions of (75) are invariant under (76). Therefore, since any solution $(\bar{x}(t), \bar{y}(t))$ of (74) is also a solution of a system of the form (75), the positive limit sets of solutions of (74) are also invariant under (76).

References

[1] A. Ng, K. Yoshihara, H. Hashimoto, L. Ngo-Phong, B.S. Kumar, A. de Ruiter, Nanosatellite mission for demonstrating formation keeping technology with aerodynamic drag, in: Proceedings of the 11th International Space Conference of Pacific basin Societies (ISCOPS), Beijing, China, 16–18 May, 2007.

[2] S.K. Balaji, A. Ng, K. Yoshihara, Flight dynamics and control of the JC2Sat-FF mission, in: Proceedings of the AAS Astrodynamics Specialist Conference, Mackinac Island, Michigan, 19–23 August 2007.

[3] R. Reynolds, G. Creamer, Global Lyapunov Control of Spin Stabilized Spacecraft, 2001. Flight Mechanics Symposium, NASA Conference Publication; 2001-209986.

[4] T.E. Holden, D.A. Lawrence, A Lyapunov design approach to magnetic nutation damping, in: Proceedings of the AIAA Guidance, Navigation and Control Conference, Portland, Oregon, 9–11 August 1999.

[5] M. Shigehara, Geomagnetic attitude control of an axisymmetric spinning satellite, Journal of Spacecraft 9 (6) (1972).

[6] A.A. Ilyin, M.Yu. Ovchinnikov, V.I. Penkov, S.A. Selivanov, Magnetic attitude control system for the Russian nano-satellite TNS-1, in: Proceedings of the 55th International Astronautical Congress, Vancouver, Canada, 2004.

[7] P.C. Hughes, Spacecraft Attitude Dynamics, Dover Publications, New York, 2004.

[8] H.K. Khalil, Nonlinear Systems, 2nd Edition, Prentice Hall, Upper Saddle River NJ, 1996.

[9] J.P. Lasalle, An invariance principle in the theory of stability, in: T. Basar (Ed.), Control Theory, Twenty-Five Seminal Papers (1932–1981), IEEE Press, New York, 2001, pp. 309–320.

[10] J.R. Wertz, Spacecraft Attitude Determination and Control, Kluwer Academic Publishers, Dordrecht, Holland, 1978.